Jeff Moehlis
Department of Mechanical Engineering,
University of California, Santa Barbara,
Santa Barbara, CA 93106
e-mail: moehlis@engineering.ucsb.edu

Eric Shea-Brown
Courant Institute for Mathematical Sciences,
and Center for Neural Science,
New York University,
New York, NY 10012
e-mail: ebrown@math.nyu.edu

Herschel Rabitz
Department of Chemistry,
Princeton University,
Princeton, NJ 08544
e-mail: hrabitz@princeton.edu

Optimal Inputs for Phase Models of Spiking Neurons

Variational methods are used to determine the optimal currents that elicit spikes in various phase reductions of neural oscillator models. We show that, for a given reduced neuron model and target spike time, there is a unique current that minimizes a square-integral measure of its amplitude. For intrinsically oscillatory models, we further demonstrate that the form and scaling of this current is determined by the model's phase response curve. These results reflect the role of intrinsic neural dynamics in determining the time course of synaptic inputs to which a neuron is optimally tuned to respond, and are illustrated using phase reductions of neural models valid near typical bifurcations to periodic firing, as well as the Hodgkin-Huxley equations. [DOI: 10.1115/1.2338654]

1 Introduction

Phase-reduced models of neurons have traditionally been used to investigate either the patterns of synchrony that result from the type and architecture of coupling [1–8] or the response of large groups of oscillators to external stimuli [9–11]. In all of these cases, the inputs to the model cells were fixed by definition of the model at the outset and the dynamics of phase models of networks or populations were analyzed in detail. The present paper takes a complementary, control-theoretic approach that is related to probabilistic "spike-triggered" methods [12]: we fix at the outset a feature of the dynamical trajectories of interest—spiking at a precise time t_1—and study the neural inputs that lead to this outcome. By computing the optimal such input, according to a measure of the input strength required to elicit the spike, we identify the signal to which the neuron is optimally "tuned" to respond. We view the present work as part of the first attempts [13,14] to understand the dynamical response of neurons using control theory, and, as we expect that insights from this general perspective will be combined with the "forward" dynamics results that Phil Holmes and many others have derived to ultimately enhance our understanding of neural processing, we hope that it will serve as a fitting tribute to his work.

2 Optimal Current for Specified Time of Firing

2.1 Problem Formulation. Consider the phase model for a spiking (i.e., firing) neuron

$$\frac{d\theta}{dt} = f(\theta) + Z(\theta)I(t) \tag{2.1}$$

where $f(\theta)$ gives the neuron's baseline dynamics, $Z(\theta)$ is its phase sensitivity function, and $I(t)$ is a current stimulus (e.g., [9,15]). We assume that $Z(\theta)$ vanishes only at isolated points, and that $f(\theta) > 0$ at these points, so orbits of full revolution are possible. Here θ is 2π periodic on $[0, 2\pi)$, and by convention $\theta = 0$ corresponds to the spiking of the neuron.

Suppose that, for a specified time t_1, for all stimuli $I(t)$ that evolve $\theta(t)$ via (2.1) from $\theta(0) = 0$ to $\theta(t_1) = 2\pi$ (that is, that cause the cell to spike at time t_1, following a spike at time 0), we want

to find the stimulus that minimizes the cost function $G[I(t)] = \int_0^{t_1} [I(t)]^2 dt$, the square-integral cost on the current. (For a system obeying Ohm's law and with resistance R, this corresponds to minimizing the power $P \sim I^2 R$.) Other choices, including costs on the time derivative of the current, lead to alternate equations below, but can be handled similarly (cf. [16]).

We apply calculus of variations to minimize [13]

$$C[I(t)] = \int_0^{t_1} \underbrace{\left\{ [I(t)]^2 + \lambda \left(\frac{d\theta}{dt} - f(\theta) - Z(\theta)I(t) \right) \right\}}_{P[I(t)]} dt \tag{2.2}$$

with λ being the Lagrange multiplier, which forces the dynamics to satisfy (2.1). The associated Euler-Lagrange equations are

$$\frac{\partial P}{\partial I} = \frac{d}{dt}\left(\frac{\partial P}{\partial \dot{I}}\right), \quad \frac{\partial P}{\partial \lambda} = \frac{d}{dt}\left(\frac{\partial P}{\partial \dot{\lambda}}\right), \quad \frac{\partial P}{\partial \theta} = \frac{d}{dt}\left(\frac{\partial P}{\partial \dot{\theta}}\right) \Rightarrow$$

$$I(t) = \frac{\lambda(t)Z[\theta(t)]}{2} \tag{2.3}$$

$$\frac{d\theta}{dt} = f(\theta) + Z(\theta)I(t) = f(\theta) + \frac{\lambda[Z(\theta)]^2}{2} \tag{2.4}$$

$$\frac{d\lambda}{dt} = -\lambda f'(\theta) - \lambda Z'(\theta)I(t) = -\lambda f'(\theta) - \frac{\lambda^2 Z(\theta)Z'(\theta)}{2} \tag{2.5}$$

where $' = d/d\theta$. To find the optimal $I(t)$, (2.4) and (2.5) need to be solved subject to the conditions $\theta(0) = 0, \theta(t_1) = 2\pi$. This requires finding the corresponding initial condition $\lambda(0) \equiv \lambda_0$, which can be done with appropriate numerical methods. The solution $(\theta(t), \lambda(t))$ using this initial condition can then be used in (2.3) to give the optimal stimulus $I(t)$. (For higher-dimensional neural models, such as the Hodgkin-Huxley equations considered below, gradient-based numerical models that iteratively update $I(t)$ via the variational derivative $\delta P / \delta I(t)$ may be required; see [16].)

Applying the Legendre transformation [17], we observe that the Hamiltonian $H(\theta, \lambda) = \lambda f(\theta) + \lambda^2 [Z(\theta)]^2 / 4$ is conserved on trajectories for the Euler-Lagrange equations (2.4) and (2.5). Taking initial conditions $(\theta, \lambda) = (0, \lambda_0)$ with $H_0 \equiv H(0, \lambda_0)$, the trajectories thus satisfy

$$\frac{\lambda^2 [Z(\theta)]^2}{4} + \lambda f(\theta) - H_0 = 0 \tag{2.6}$$

2.2 Existence and Uniqueness of Optimal Inputs $I(t)$. As mentioned above, the trajectories of interest are orbits that go from $\theta=0$ to $\theta=2\pi$ over the timespan $[0,t_1]$. We now show that there is a unique such orbit and, hence, input $I(t)$, which is optimal in the sense introduced above. We refer to this orbit as the *optimal trajectory*. First, we make two assumptions:

$$Z(0)=0, \quad f(0)>0 \qquad (2.7)$$

That is, we assume that the phase sensitivity function $Z(\cdot)$ vanishes at the spike phase $\theta=0$ and that the intrinsic phase dynamics are increasing at this point. These conditions are required for well-defined phase reductions of spiking neurons [9], as they ensure that the spike phase is not crossed "backwards."

LEMMA 2.1. *Assume that* (2.7) *holds. Then* $d\theta/dt>0$ *for any trajectory of* (2.4) *or* (2.5) *with* $\theta(0)=0$ *and* $\theta(\tau)=2\pi$.

Proof. Consider a trajectory $\{(\theta(t),\lambda(t))\}$, $0\le t\le\tau$, which solves (2.4) and (2.5). From (2.7), we have $(d\theta/dt)|_{t=0}>0$. Assume in point of contradiction that there exists a time $0<\hat{t}<\tau$ such that $(d\theta/dt)|_{t=\hat{t}}<0$. Since $\theta(\tau)=2\pi$, in this case there also exists a phase $\bar{\theta}<2\pi$ such that $\theta(t)=\bar{\theta}$ for three distinct times between 0 and τ. A quick sketch in the (θ,λ) plane shows that, since any trajectory $\{(\theta(t),\lambda(t))\}$ is not self-intersecting, the trajectory under our assumption contains three distinct points $(\bar{\theta},\lambda_j)$, $j=1,2,3$. However, the trajectory must also be a level set of the Hamiltonian; from (2.6), which is quadratic in $\lambda(\theta)$, such a level set contains at most two points $(\theta,\lambda(\theta))$ for any value of θ. Therefore, a contradiction has been reached and the lemma follows. $\square$

LEMMA 2.2. *Assume that* (2.7) *holds. For a solution to* (2.4) *and* (2.5)

$$\lambda(\theta)[Z(\theta)]^2 = 2[-f(\theta) + \sqrt{[f(\theta)]^2 + [Z(\theta)]^2 H_0}] \qquad (2.8)$$

Proof. Multiplying (2.6) by $[Z(\theta)]^2$ and solving the resulting quadratic equation in $\lambda(\theta)[Z(\theta)]^2$ gives

$$\lambda(\theta)[Z(\theta)]^2 = 2[-f(\theta) \pm \sqrt{[f(\theta)]^2 + [Z(\theta)]^2 H_0}]$$

However, (2.4) shows that $d\theta/dt<0$ whenever $\lambda(\theta)[Z(\theta)]^2/2<-f(\theta)$. Therefore, from Lemma 2.1, we see that optimal solutions only follow the "plus" branch.

Now, we give the main result of this section.

PROPOSITION 2.3. *Assume that* (2.7) *holds. Then for any* $t_1>0$, *an optimal trajectory exists and is unique.*

Proof. Using Lemma 2.2 to rewrite Eq. (2.4), we see that there exist optimal solutions with spike times t_1 given by

$$t_1 = \int_0^{t_1} dt = \int_0^{2\pi} \frac{d\theta}{f(\theta) + \frac{\lambda[Z(\theta)]^2}{2}} = \int_0^{2\pi} \frac{d\theta}{\sqrt{[f(\theta)]^2 + [Z(\theta)]^2 H_0}} \qquad (2.9)$$

Differentiating, we have

$$\frac{\partial t_1}{\partial H_0} = -\frac{1}{2}\int_0^{2\pi} \frac{[Z(\theta)]^2 d\theta}{\{[f(\theta)]^2 + [Z(\theta)]^2 H_0\}^{3/2}} < 0 \qquad (2.10)$$

provided $[f(\theta)]^2 + [Z(\theta)]^2 H_0 > 0$, which is necessary for (2.8) to give a valid trajectory. Thus, t_1 decreases monotonically as H_0 increases. Noting that λ_0 varies monotonically with H_0 under our assumptions (2.7) (in fact, $H_0 = f(0)\lambda_0$), we conclude that there is at most one value of λ_0 that gives a trajectory with a particular t_1. Examining (2.9) and recalling our assumption from the outset that $Z(\theta)$ vanishes only at isolated points, and that $f(\theta)>0$ at these points, we see that (i) by choosing H_0 (and, hence, λ_0) to be arbitrarily large, an optimal trajectory with arbitrarily small t_1 may be found; (ii) by choosing H_0 to approach $\sup_\theta(-[f(\theta)]^2/[Z(\theta)]^2)$ from above, an optimal trajectory with arbitrarily large t_1 may be found. $\square$

2.3 Intrinsically Oscillatory Neurons. For the special case that $f(\theta)=\omega=$const, so that the neuron fires periodically with period $T=2\pi/\omega$ in the absence of input $I(t)$, $Z(\theta)$ is called the phase response curve (PRC). Then, (2.4) and (2.5) have fixed points (θ_f,λ_f) that satisfy $Z'(\theta_f)=0, \lambda_f=-2\omega/[Z(\theta_f)]^2$. The eigenvalues of the Jacobian evaluated at these fixed points are $\pm\omega\sqrt{-Z''(\theta_f)/Z(\theta_f)}$. If $Z''(\theta_f)$ and $Z(\theta_f)$ have opposite signs, such a fixed point is a saddle point. The associated stable and unstable manifolds are found to be trajectories with $H_0 = H(\theta_f,\lambda_f) = -\omega^2/[Z(\theta_f)]^2$.

2.3.1 Form of Optimal Current for Small $|t_1-T|$. Suppose $f(\theta)=\omega>0$, $Z(0)=0$, and that the desired spike time t_1 is close to the natural period T. We can then solve (2.4) and (2.5) to lowest order in $|t_1-T|$ explicitly, demonstrating that in this case the optimal current is proportional to the PRC. Thus, the PRC determines the inputs that neurons are naturally tuned to, in the sense of the optimization problem at hand.

First note that the line $\lambda=0$ is invariant for (2.4) and (2.5), and corresponds to $d\theta/dt=\omega$ and, hence, to $t_1=T$. From (2.3), we see that $I(t)=0$ in this case; this is expected because no control is required for an intrinsically oscillatory neuron to fire a spike at its natural period. For $t_1\approx T$, we Taylor expand t_1 with respect to the initial condition $\lambda(0)$ to give $t_1 = T + (\partial t_1/\partial\lambda(0)|_{\lambda(0)=0})\lambda(0)$ to lowest order in (t_1-T). Thus, the initial λ value needed to give a trajectory that reaches $\theta=2\pi$ at time t_1 is $\lambda(0)\approx(t_1-T)/[\partial t_1/\partial\lambda(0)]|_{\lambda(0)=0}$, to lowest order in t_1-T. From (2.10), noting for $Z(0)=0$ that $\lambda(0)=H_0/\omega$, we then have

$$\lambda(0) = -\frac{t_1-T}{\omega \left.\frac{\partial t_1}{\partial H_0}\right|_{H_0=0}} = -\frac{(t_1-T)2\omega^2}{\int_0^{2\pi} [Z(\theta)]^2 d\theta} \qquad (2.11)$$

Letting $t_1-T=\mathcal{O}(\varepsilon)$ and expanding

$$\lambda(t) = \lambda^{(0)}(t) + \varepsilon\lambda^{(1)}(t) + \varepsilon^2\lambda^{(2)}(t) + \cdots \qquad (2.12)$$

$$\theta(t) = \theta^{(0)}(t) + \varepsilon\theta^{(1)}(t) + \varepsilon^2\theta^{(2)}(t) + \cdots \qquad (2.13)$$

we find from Eqs. (2.4) and (2.5) that $\lambda^{(0)}=0$ and $\lambda^{(1)}(t)=\lambda(0)/\varepsilon+O(\varepsilon)$. Furthermore, $\theta^{(0)}=\omega t$. Therefore, from (2.3), the optimal current is given by

$$I(t) = \frac{1}{2}\lambda(0)Z(\theta^{(0)}) + O((t_1-T)^2) \qquad (2.14)$$

$$= -\frac{(t_1-T)\omega^2 Z(\omega t)}{\int_0^{2\pi} [Z(\theta)]^2 d\theta} + O((t_1-T)^2) \qquad (2.15)$$

Finally, we note that it is expected that since $Z(0)=Z(2\pi)=0$, the optimal current should vanish for $\theta=0$ (at $t=0$) and $\theta=2\pi$ (at $t=t_1$). This is not the case for (2.15). However, letting $Z(\omega t) \to Z(\omega t-2\pi t(t_1-T)/(t_1 T))=Z(\omega t T/t_1)$, which changes only the $O((t_1-T)^2)$ terms in (2.15), we obtain an approximation which satisfies these conditions. With this in mind, to lowest order in t_1-T, we approximate the optimal current that causes the neuron to spike at $t_1\approx T$ as

$$I(t) = -\frac{(t_1-T)\omega^2 Z(\omega t - 2\pi t(t_1-T)/(t_1 T))}{\int_0^{2\pi} [Z(\theta)]^2 d\theta} + O[(t_1-T)^2] \qquad (2.16)$$

2.3.2 Scaling of Optimal Current for Small $|t_1-T|$. In [9], it is shown how PRCs for phase reductions of neural oscillators near common bifurcations to periodic firing scale with the baseline
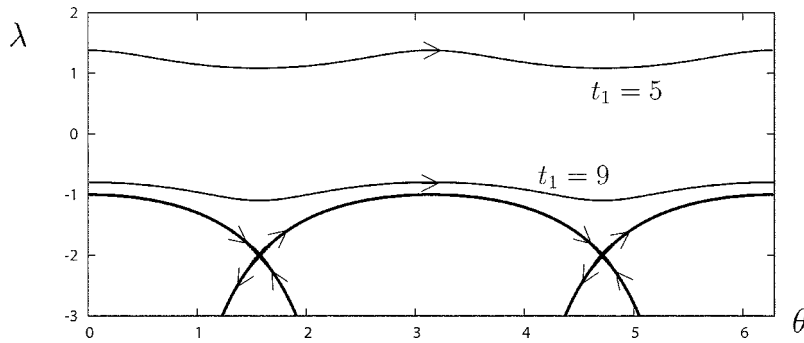
Fig. 1 Phase space for (2.4) and (2.5) with the sinusoidal PRC (3.19) and $\omega = Z_d = 1$, showing fixed points at $(\theta, \lambda) = (\pi/2, -2)$ and $(3\pi/2, -2)$, stable and unstable manifolds of the fixed points, and trajectories with $t_1 = 5$ and $t_1 = 9$

firing frequency ω. These reductions have the form $Z(\theta) = Z_d(\omega)\tilde{Z}(\theta)$, where the coefficient $Z_d(\omega)$ captures the scaling with ω. For example, for neurons near a saddle node on a periodic orbit (SNIPER) bifurcation, $Z(\theta) = (c/\omega)[1 - \cos(\theta)]$ (cf. [18]), where c is a model-dependent constant, so $Z_d(\omega) = 1/\omega$; for neurons near a supercritical Hopf transition, $Z(\theta) = (c/\sqrt{\omega - \omega_H})\sin(\theta)$ (cf. [19]), where ω_H is the frequency at the bifurcation; thus, $Z_d(\omega) = 1/\sqrt{\omega - \omega_H}$.

Using these results and (2.16), it is readily determined how the optimal $I(t)$ scales with ω when the desired spike time t_1 is a (fixed) small perturbation from the natural period $T = 2\pi/\omega$. Denoting by I_{max1} the maximum of $|I(t)|$ in this case, we get

$$I_{max1} = c_1 \omega^2 / Z_d(\omega) \qquad (2.17)$$

for a fixed neuron model and time shift $t_1 - T$, to lowest order in $t_1 - T$. Here, c_1 is a model-dependent constant. In words, Eq. (2.17) shows how the amplitude of the optimal current required to perturb spike times by a fixed amount scales with the baseline frequency of the neuron. A complementary relationship is obtained by asking how this amplitude scales with baseline frequency when the optimal current perturbs the spike time by a fixed fraction of the (varying) baseline period. In this case, setting $t_1 - T$ in (2.16) to pT, where p is the fixed fraction, gives

$$I_{max2} = c_2 \omega / Z_d(\omega) \qquad (2.18)$$

For phase reductions near the SNIPER bifurcation, and for other cases in which $Z_d(\omega)$ decreases as ω increases, both expressions (2.17) and (2.18) demonstrate that the optimal currents required to perturb spike times diminish rapidly in amplitude at lower baseline frequencies. We will return to this point below.

3 Examples

3.1 Sinusoidal PRC. Consider $f(\theta) = \omega = $ const and the PRC

$$Z(\theta) = Z_d \sin(\theta) \qquad (3.19)$$

where Z_d is a constant. This might arise due to proximity to a supercritical Hopf or a Bautin bifurcation [9,19]. There are fixed points of the Euler-Lagrange equations (2.4) and (2.5) at $(\theta_f, \lambda_f) = (\pi/2, -2\omega/Z_d^2), (3\pi/2, -2\omega/Z_d^2)$, each with eigenvalues ω and $-\omega$. The phase space for (2.4) and (2.5) is shown in Fig. 1 for $\omega = Z_d = 1$. We integrate (2.9) to give

$$t_1 = \frac{4}{\omega} K\left(-\frac{H_0 Z_d^2}{\omega^2}\right) = \frac{4}{\omega} K\left(-\frac{\lambda_0 Z_d^2}{\omega}\right) \qquad (3.20)$$

Here, $K(x)$ is the complete elliptic function of the first kind, a monotonically increasing function with properties that

$$K(0) = \frac{\pi}{2}, \quad \lim_{x \to -\infty} K(x) = 0, \quad \lim_{x \to 1} K(x) = \infty \qquad (3.21)$$

Figure 2 shows how t_1 depends on λ_0; as expected from (2.10), it decreases monotonically as λ_0 increases. Furthermore, as expected from Sec. 2.3, the initial condition $\lambda_0 = 0$ gives $t_1 = 2\pi/\omega$. Finally, from (3.20) and (3.21), we see that t_1 blows up to infinity as $H_0 \to -\omega^2/Z_d^2$; this is expected from (2.9), as $-\omega^2/Z_d^2 = \sup_\theta(-[f(\theta)]^2/[Z(\theta)]^2)$. This corresponds to approach toward the stable and unstable manifolds of the fixed points. This forces the trajectory to spend asymptotically long times near the fixed points (with corresponding current approximately given by (2.3) evaluated at the fixed point), delaying its arrival to $\theta = 2\pi$,

To obtain the initial condition λ_0 for a particular value of t_1, one can in principle invert the function $K(x)$ in (3.20). In practice, it is easier to solve (2.4) and (2.5) subject to the conditions $\theta(0) = 0, \theta(t_1) = 2\pi$ numerically using a shooting method. We used such a method to generate the optimal currents for $\omega = Z_d = 1$ for various values of t_1 shown in Fig. 3, where the time axis has been scaled for ease of comparison. Not surprisingly, if we want the neuron to fire more quickly than it would in the absence of the stimulus (i.e.,
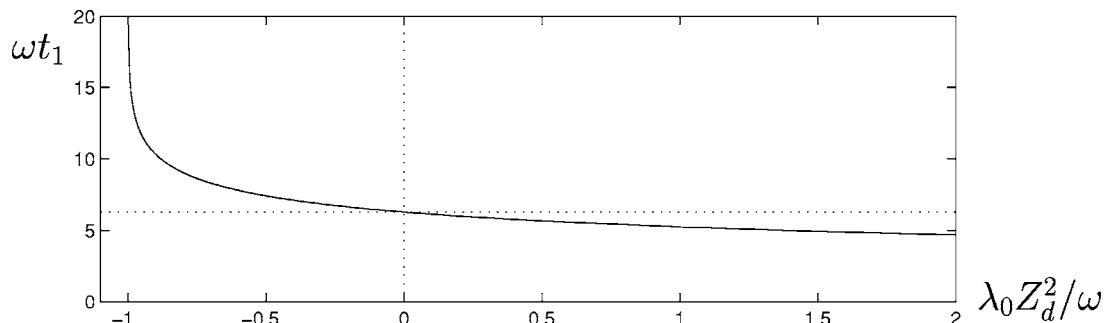

Fig. 2 Dependence of t_1 on λ_0 for the sinusoidal PRC (3.19), as obtained from (3.20)
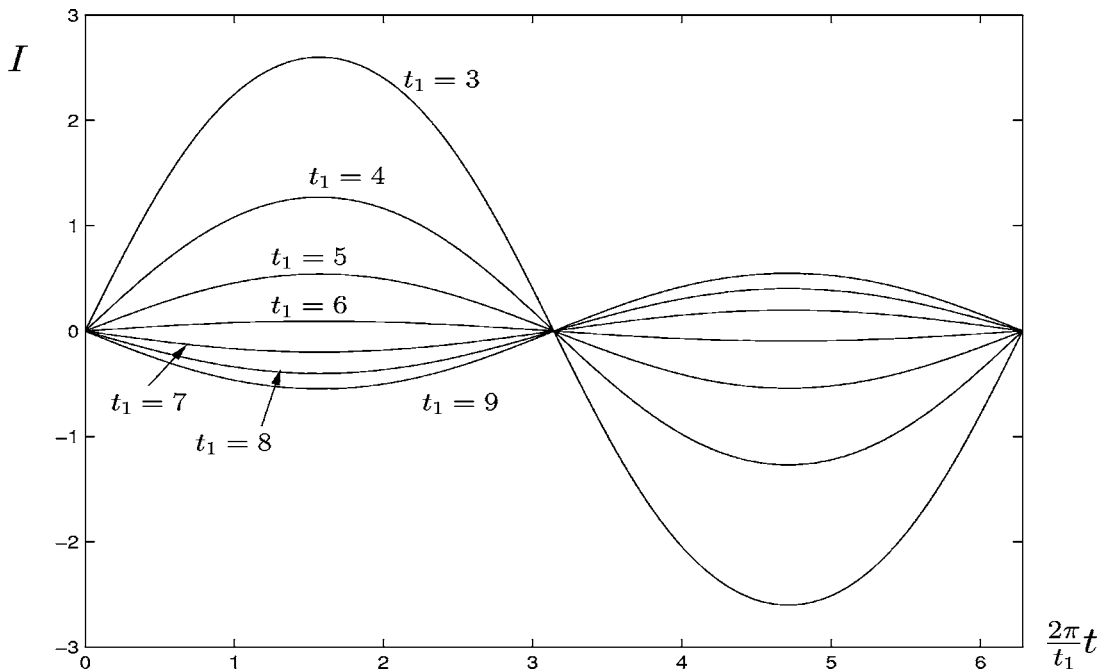
Fig. 3 Optimal currents for the sinusoidal PRC (3.19) with $\omega = Z_d = 1$ for different values of t_1, with scaled time axis for ease of comparison

if $t_1 < T$), then the optimal current is positive (respectively, negative) for θ values for which $Z(\theta)$ is positive (respectively, negative). Furthermore, it is clear that the approximation (2.15) characterizes optimal currents for $t_1 \approx T$ (Fig. 4(a)), and that the optimal current scales as expected with ω (Fig. 5(a)).

3.2 SNIPER PRC. Consider $f(\theta) = \omega = $ const, and the PRC

$$Z(\theta) = Z_d(1 - \cos \theta) \qquad (3.22)$$

This could arise for neurons near a SNIPER bifurcation (i.e., a saddle-node bifurcation on a periodic orbit) [9,18]. Here, there is

one fixed point of the Euler-Lagrange equations (2.4) and (2.5) at $(\theta_f, \lambda_f) = [\pi, -\omega/(2Z_d^2)]$, with eigenvalues $\pm \omega/\sqrt{2}$. The phase space for (2.4) and (2.5) for this PRC is shown in Fig. 6 for $\omega = 1$ and $Z_d = 1$. We again used a shooting method to find the optimal currents—a comparison for various values of t_1 is given in Fig. 7. Again, (2.15) is a good approximation for $t_1 \approx T$ (see Fig. 4(b)), and the expected scaling of optimal currents with ω is seen (Fig. 5(b)).

3.3 Theta Neuron. The "theta neuron" model describes both
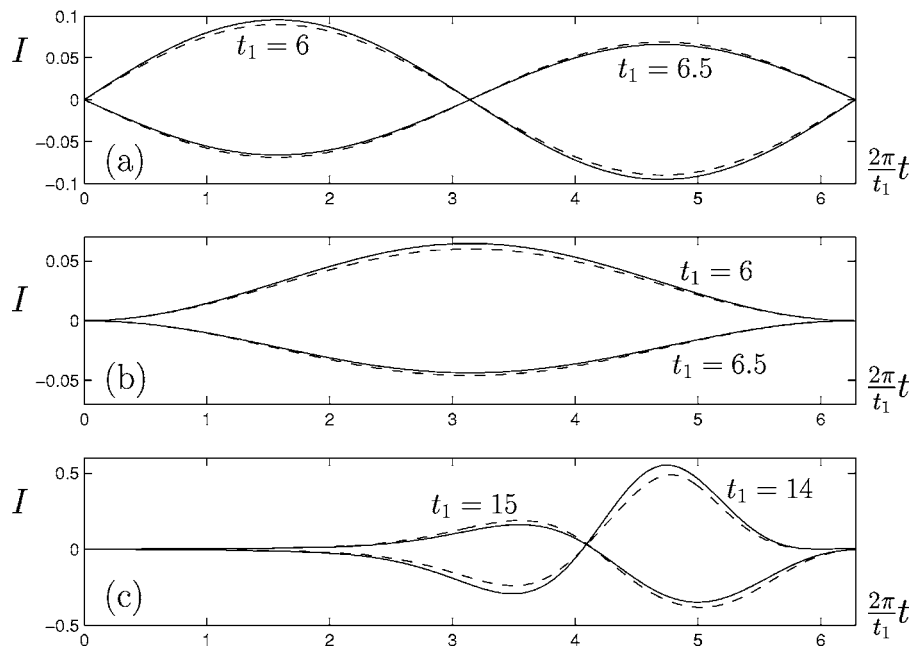

Fig. 4 Exact (solid lines) and approximate (dashed lines) optimal currents for t_1 as labeled with (a) the sinusoidal PRC (3.19) with $\omega = Z_d = 1$, (b) the SNIPER PRC (3.22) with $\omega = Z_d = 1$, and (c) the PRC corresponding to the Hodgkin-Huxley equations with $I_b = 10$
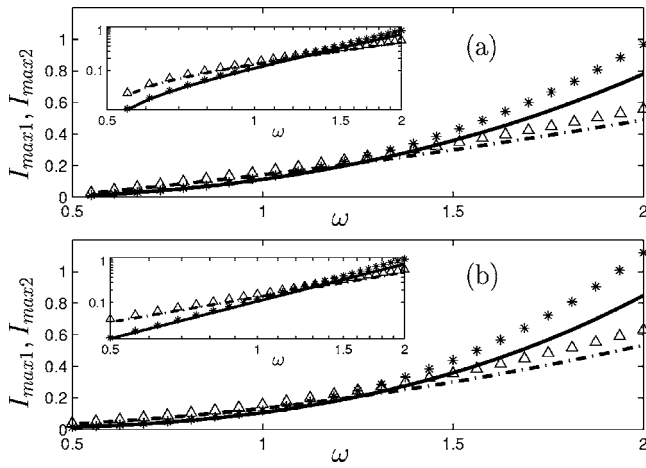
Fig. 5 Scaling of the amplitude of optimal currents with baseline frequency ω, for (a) the sinusoidal PRC $Z(\theta)$ $=(1/\sqrt{\omega-\omega_H})\sin(\theta)$, with $\omega_H=0.5$ and (b) the SNIPER PRC $Z(\theta)$ $=(1/\omega)[1-\cos(\theta)]$. For $t_1-T=-0.5$, the amplitude I_{max1} from the lowest-order expression (2.17) is given by solid lines; stars give the analogous numerically computed values (i.e., to all orders). For the fraction $p=0.9$, the amplitude I_{max2} from the lowest-order expression (2.18) is given by dotted-dashed lines; triangles give the analogous numerical values. Insets give the same data on log-log axes.

superthreshold and subthreshold dynamics near a SNIPER bifurcation [18]. With our control current $I(t)$, this model is

$$\frac{d\theta}{dt} = 1 + \cos\theta + (1-\cos\theta)(I(t)+I_b) \qquad (3.23)$$

i.e., Eq. (2.1) with $f(\theta)=1+\cos\theta+I_b(1-\cos\theta)$, $Z(\theta)=1-\cos\theta$. As above, θ is 2π periodic and spikes fire at $\theta=0$. If the baseline current $I_b>0$, then the cell fires periodically in the absence of input $I(t)$, with angular frequency $\omega=2\sqrt{I_b}$. If $I_b<0$, then the model is excitable: no spikes occur without input $I(t)$, as there are two fixed points (one of which is stable) for $I(t)=0$; however, for appropriate inputs $I(t)$ spikes can occur. When $I_b>0$, applying the coordinate transformation $\theta(\phi)=2\tan^{-1}[\sqrt{I_b}\tan(\phi/2-\pi/2)]+\pi$ to (3.23) gives $d\phi/dt=\omega+\frac{2}{\omega}(1-\cos\phi)I(t)$, i.e., the governing equation for the SNIPER PRC with $Z_d=2/\omega$. This transformation preserves $\theta(\phi=0)=0$ and $\theta(\phi=2\pi)=2\pi$, i.e., the property of spiking at 0 and 2π.

The Euler-Lagrange equations (2.4) and (2.5) for the theta neuron model have a fixed point at $(\theta_f,\lambda_f)=(\pi,-I_b)$, with eigenvalues $\pm\sqrt{2I_b}$. For $I_b<0$, they also have fixed points at (θ_f,λ_f)

$=(\cos^{-1}[(I_b+1)/(I_b-1)],0)$, with eigenvalues $\pm2\sqrt{-I_b}$. The phase space for the Euler-Lagrange equations for this model with I_b $=0.25$ and $I_b=-0.25$ is shown in Fig. 8. For large t_1 when $I_b<0$, the solution spends most of its time near one of the two saddle points, with an increasingly punctate current pulse peaked halfway through its transit from $\theta=0$ to $\theta=2\pi$, as Fig. 9 shows.

3.4 Hodgkin-Huxley PRC. The Hodgkin-Huxley equations [20] are a system of four ordinary differential equations (ODEs) that model the generation of action potentials (i.e., spikes) in the squid giant axon, based on the dynamical interplay between ionic conductances and intracellular voltage. They have been highly influential, with most mathematical neuron models being based on them in one way or another. Here we consider the Hodgkin-Huxley equations with standard parameters and applied baseline current $I_{HH}=10$, for which the neuron fires periodically with period $T=14.63$ ms, corresponding to $\omega=0.429$ rad/ms. The PRC for this system, computed numerically with the software X-Windows Phase Plane (XPP) [21], is shown in Fig. 10. To numerically study the Euler-Lagrange equations, we approximated the PRC obtained from XPP as a Fourier series with 21 terms. It is found numerically that the Euler-Lagrange equations (2.4) and (2.5) for this PRC have fixed points at $(\theta,\lambda)=(3.53,-74.73)$ and $(4.89,-18.11)$, both saddles with eigenvalues approximately equal to ±0.92. The phase space for (2.4) and (2.5) for this PRC is shown in Fig. 11. We used a shooting method to find the optimal currents shown in Fig. 12 for various values of t_1.

It is natural to ask to what extent the optimal current found using the phase model with this Hodgkin-Huxley PRC causes a neuron described by the *full* equations to fire at the specified time. To answer this, we take initial conditions for the Hodgkin-Huxley equations following a spike, apply the optimal $I(t)$ found from the phase model until the specified time t_1, then allow the full equations to evolve under their natural dynamics without injected current. We measure the firing time as the time of the first peak in the voltage above an appropriate threshold.

For t_1 close to the intrinsic period, the Hodgkin-Huxley equations with these inputs fire at approximately the specified times t_1 (in microseconds); see Fig. 13 for $t_1=14$. In this case, $|I(t)|$ remains relatively small, which is necessary for the phase model to accurately characterize the full Hodgkin-Huxley equations (e.g., [9]). As t_1 moves away from the natural period, the optimal current from the phase model causes the full equations to spike later than the target time, as $|I(t)|$ becomes relatively large and the phase reduction loses validity. In fact, simulations show that this $I(t)$ pushes the trajectory near an unstable fixed point (not captured by the phase model) having complex eigenvalues with small, positive real parts. The time required for the trajectory to spiral away from this fixed point accounts for some of the discrepancy with the phase model. Figure 14 compares the specified time
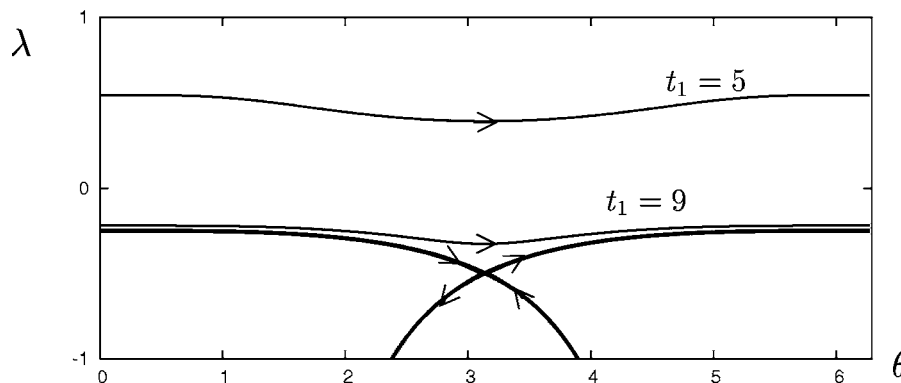

Fig. 6 Phase space for (2.4) and (2.5) for the SNIPER PRC (3.22) with $\omega=1$ and $Z_d=1$, showing the fixed point at $(\theta,\lambda)=(\pi,-1/2)$, stable and unstable manifolds of the fixed point, and trajectories for periodic orbits with period $t_1=5$ and $t_1=9$
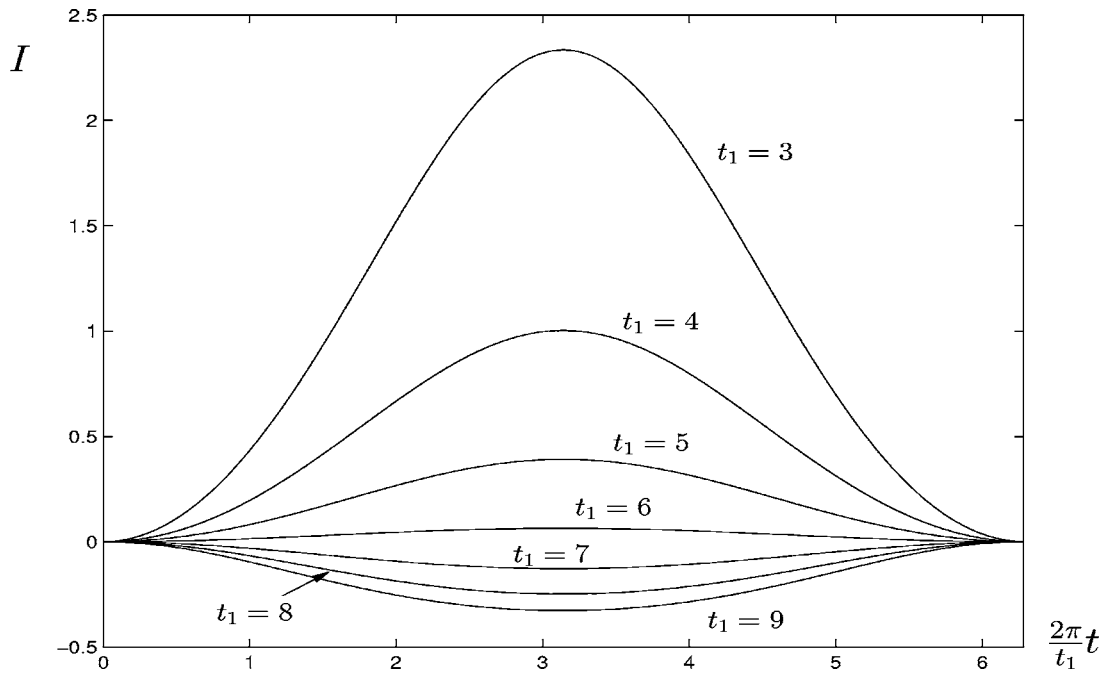
Fig. 7 Optimal currents for the SNIPER PRC (3.22) with $\omega=Z_d=1$ for different values of t_1, with scaled time axis for ease of comparison
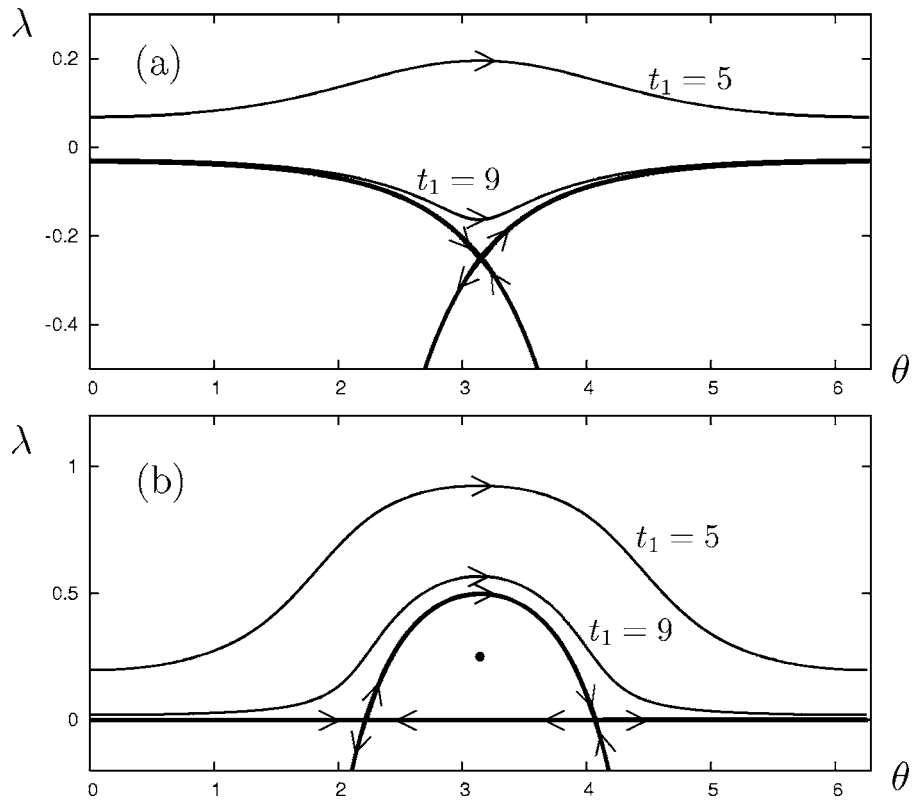

Fig. 8 Phase space for (2.4) and (2.5) for the theta neuron model (3.23) with (a) I_b =0.25, (b) I_b=−0.25, showing fixed points, stable and unstable manifolds of the fixed points, and trajectories for periodic orbits with period t_1=5 and t_1=9. The dot in (b) is a center fixed point.
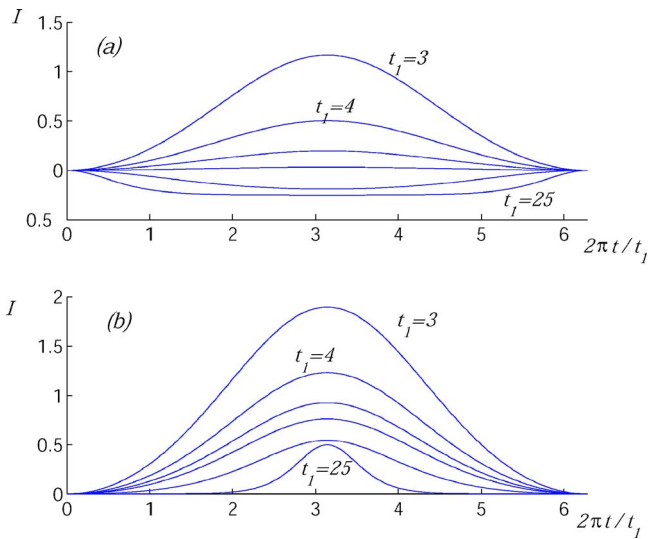
Fig. 9 Optimal currents for the theta neuron model, (*a*) with $I_b=0.25$ and (*b*) with $I_b=-0.25$, with time axis scaled as above. Target time values are, from top, $t_1=3,4,5,6,10,25$.

of firing t_1 and the actual time of firing t_1^{HH} for the full Hodgkin-Huxley equations, using the current found from optimizing the phase model.

4 Optimal Current for Minimizing the Time of Firing

The previous sections were concerned with determining the optimal current to cause a neuron described by a phase model to fire at a specified time. Here, we consider optimizing the current, subject to the constraint that $|I(t)| \leq \bar{I}$ for all t, which causes the

neuron described by a phase model to fire as quickly as possible. This constraint could represent the maximal possible synaptic input that upstream neurons can provide to the neuron at hand. Here, we do not constrain the rate with which $I(t)$ can vary; in practice, the timescale of the synaptic currents, which varies among synapse types but can be very rapid, determines the viability of this assumption of unconstrained rate.

The following argument suggests using "bang-bang control," in which the injected current takes the extreme values of $\pm\bar{I}$ [16]. From (2.1), in a time step dt the phase advances by

$$d\theta = [f(\theta) + Z(\theta)I(t)]dt \qquad (4.24)$$

To get the neuron to fire as quickly as possible, we maximize $d\theta$ at each timestep. Clearly, to do this we should take

$$I(t) = I^{bb}[\theta(t)] = \begin{cases} \bar{I} & \text{for } Z[\theta(t)] > 0 \\ -\bar{I} & \text{for } Z[\theta(t)] < 0 \end{cases} \qquad (4.25)$$

More completely, suppose that the neuron starts with initial phase θ_i. It will fire at time t_f given by

$$t_f = \int_0^{t_f} dt = \int_{\theta_i}^{2\pi} \frac{d\theta}{f(\theta) + Z(\theta)I(t)} \qquad (4.26)$$

where we assume that $f(\theta) + Z(\theta)I(t)$ is always positive (if not, then from (4.24) the phase does not advance). Now, if $-|Z(\theta)|\bar{I} < Z(\theta)I(t) < |Z(\theta)|\bar{I}$, that is, the current $I(t)$ satisfies the amplitude constraint and is not given by (4.25),

$$\frac{1}{f(\theta) + Z(\theta)I(t)} > \frac{1}{f(\theta) + |Z(\theta)|\bar{I}} > 0 \qquad (4.27)$$
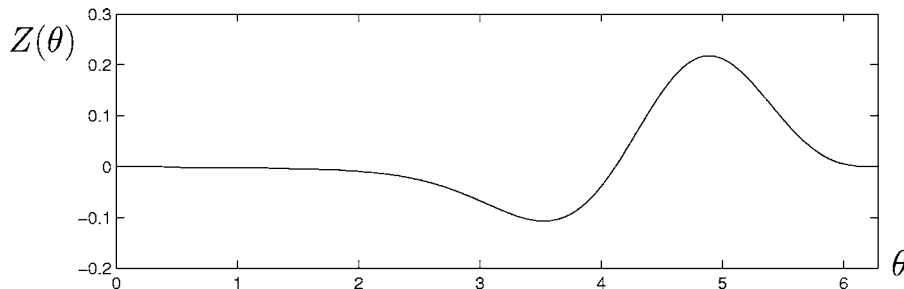

Fig. 10 Phase response curve for the Hodgkin-Huxley equations with standard parameters and injected baseline current $I_{HH}=10$
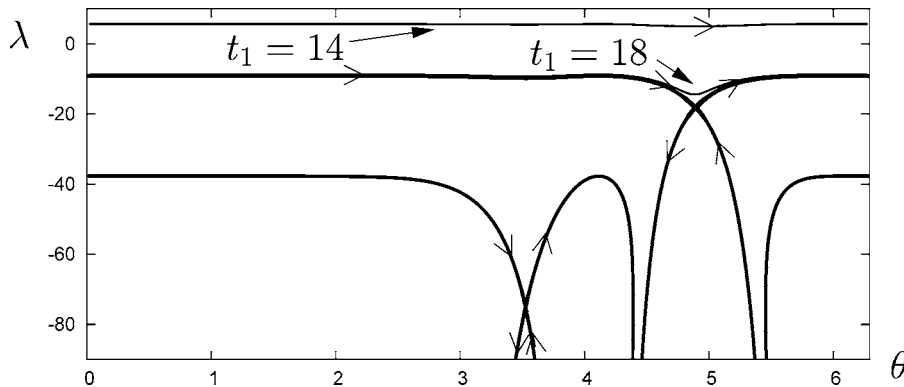

Fig. 11 Phase space for (2.4) and (2.5) for the PRC corresponding to the Hodgkin-Huxley equations with $I_{HH}=10$, showing the stable and unstable manifolds of the two fixed points, and trajectories for periodic orbits with period $t_1=14$ and $t_1=18$
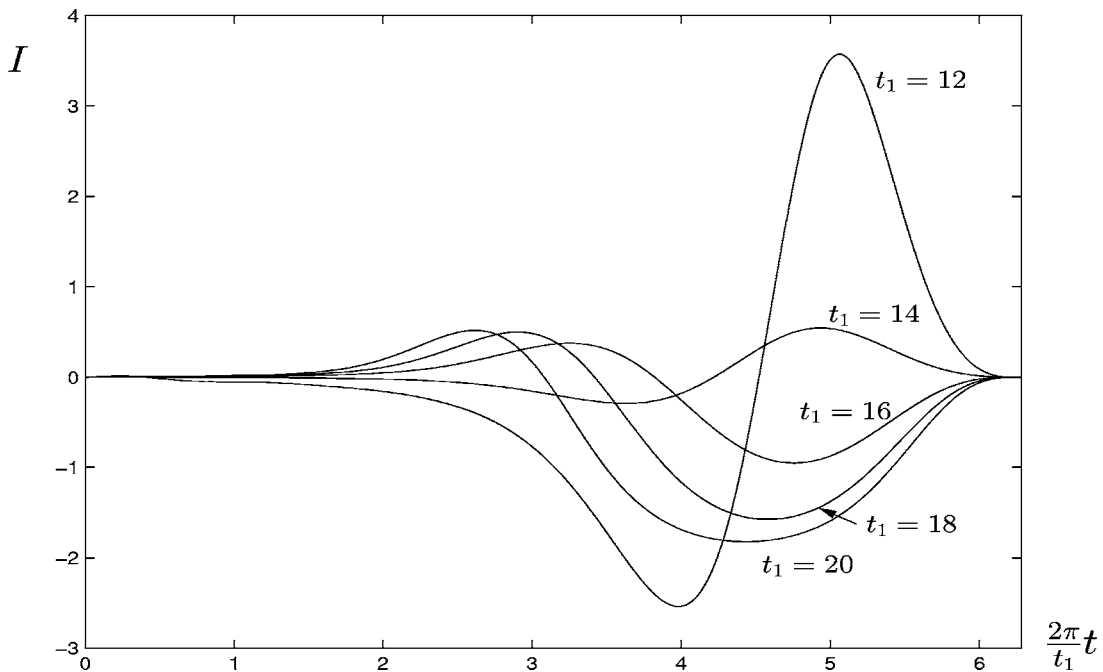
Fig. 12 Optimal currents for the PRC for the Hodgkin-Huxley equations with standard parameters and with I_{HH}=10 for different values of t_1, with scaled time axis for ease of comparison

$$\Rightarrow t_f = \int_{\theta_i}^{2\pi} \frac{d\theta}{f(\theta) + Z(\theta)I(t)} > \int_{\theta_i}^{2\pi} \frac{d\theta}{f(\theta) + Z(\theta)I^{bb}(\theta)} \equiv t_f^{bb}$$

(4.28)

where t_f^{bb} is the time the neuron fires for the current given by (4.25). Note that for bang-bang control to work, it is necessary

that $f(\theta) + |Z(\theta)|\bar{I} > 0$ for all θ. Figure 15 shows t_f^{bb} for $\theta_i = 0$ for the PRCs considered in Sec. 3. For all except the theta neuron model with negative I_b, for which one needs $\bar{I} > -I_b$ in order for bang-bang control to produce a spike, we see that t_f^{bb} approaches the natural period as $\bar{I} \to 0$, as expected.
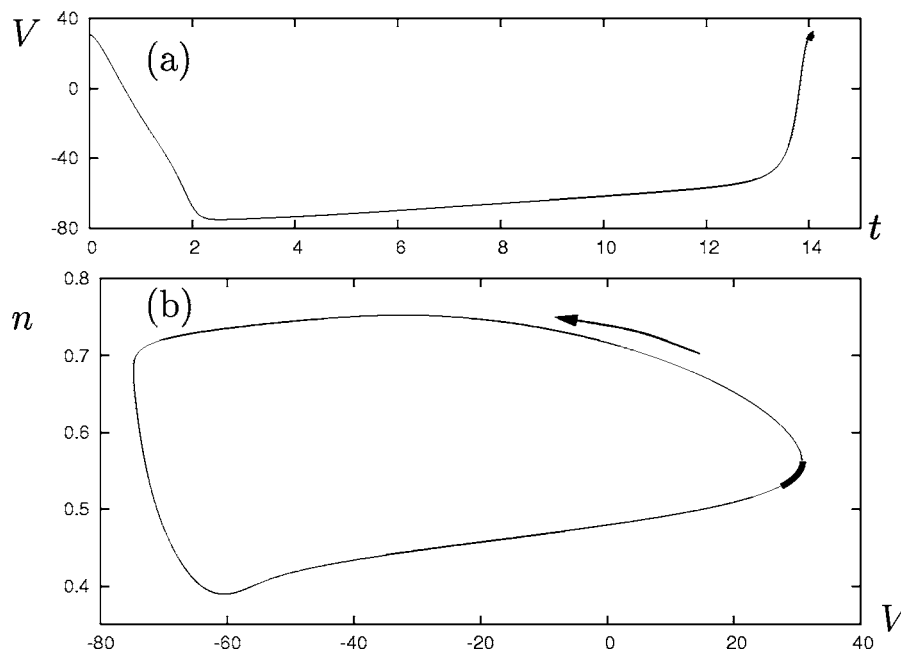

Fig. 13 Dynamics of the full Hodgkin-Huxley equations with $I(t)$ chosen to be the optimal current stimulus for t_1=14 for the phase model with the Hodgkin-Huxley PRC for I_{HH}=10. (a) shows the time series of the transmembrane voltage V, and (b) shows the phase space projection onto the (V,n) plane, where V is the voltage and n is a gating variable (using the standard Hodgkin-Huxley notation). The thin line shows the dynamics while $I(t)$ is being applied up to time t_1. The thick line shows the dynamics after $I(t)$ is turned off until the neuron first fires.
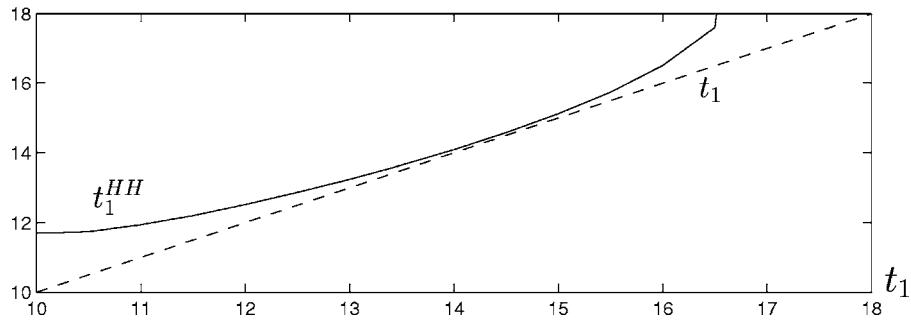
Fig. 14 Comparison of the specified time of firing t_1 and the actual time of firing t_1^{HH} for the full Hodgkin-Huxley equations for the current found from optimizing the phase model. The dashed line corresponds to exact agreement.

5 Discussion and Conclusion

In this paper, we first show that there is a unique optimal current $I(t)$ that will elicit a spike at a specified time t_1 for phase-reduced neural models satisfying a general set of conditions. We then derive results about this current $I(t)$ for intrinsically oscillatory models, using the formalism of PRCs. In particular, for these models we show that the time course of the optimal current will be proportional to the PRC itself for small perturbations in spike times. This fact, coupled with earlier results about the typical scaling of PRCs, enables us to study how the amplitude of this current scales with the baseline (i.e., unperturbed) frequency of the oscillatory model. Finally, we discuss bang-bang control, computing the earliest spike times that can be elicited in different neural models by currents of fixed maximal amplitude. All of these results are illustrated with phase-reduced neural models valid near the SNIPER and Hopf bifurcations, and with a numerically derived phase model for the Hodgkin-Huxley equations.

Our results on the form and scaling of optimal currents $I(t)$ address the question of how the dynamics of individual neurons determine the processing of synaptic inputs to produce spikes. Specifically, they imply that the standard classification of a neuron's PRC as Type I versus Type II [18] depending, respectively, on whether it is nonnegative (as for the SNIPER PRC) or takes both positive and negative values (as for the sinusoidal PRC), also determines, respectively, whether purely excitatory synapses or a

mixture of excitatory and inhibitory synapses are required to optimally adjust its spike times. As previous work [9,18,19] shows that PRCs remain invariant in form but typically increase in amplitude as baseline oscillation frequencies decrease, we also conclude that the optimal inputs for a given neuron operating at different frequencies are determined by rescaling in both time and amplitude as a *single* curve of a given form. For the standard neural models studied here, the amplitude of the current that optimally causes a fixed perturbation in spike times decreases rapidly with the model's baseline frequency, indicating increased sensitivity at low firing rates. This type of increased sensitivity, or *gain*, at lower firing rates has been emphasized in the context of population-averaged firing rates in [9,22], and is extended here to the spike times of individual neurons.

In the context of many of the neural inputs that occur in vivo, the present results may nonetheless be viewed as rather limited, as many neurons receive inputs from up to thousands of afferent synapses and the combined currents contain components distinct from the optimal inputs considered here. One approach to this more general problem is to compute time-dependent components, or 'features,' of neural inputs whose combined strengths determine whether or not a given input will elicit a spike (see [12] and references therein). In particular, [23] shows that only a few such components are required to make this determination to quite high accuracy for the Hudgkin-Huxley (HH) equations. It will be inter-
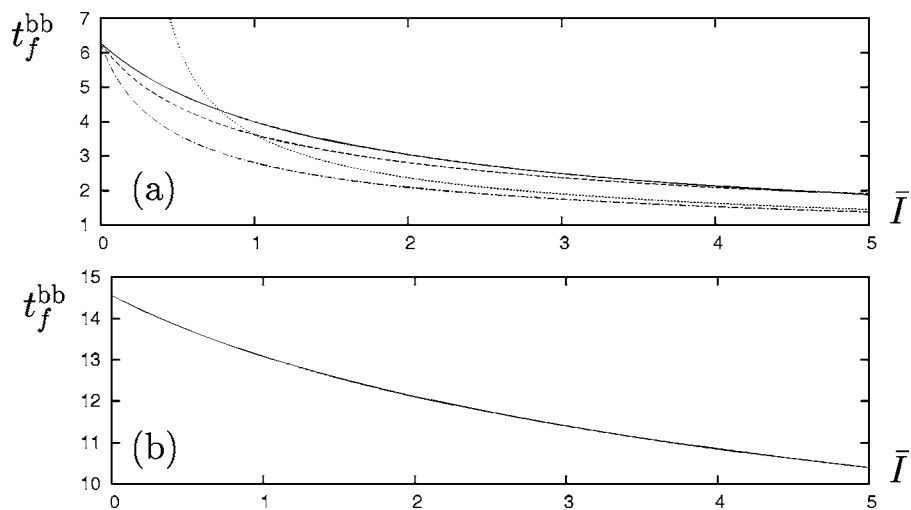

Fig. 15 Minimal time of firing t_f^{bb} as a function of $\bar{I}$, obtained using bang-bang control, for phase models starting at $\theta_i=0$ for (a) solid line: $f(\theta)=\omega=1$, $Z(\theta)=\sin\theta$; dashed line: $f(\theta)=\omega=1$, $Z(\theta)=1-\cos\theta$; dotted-dashed line: the theta neuron model with $I_b=0.25$; dotted line: the theta neuron model with $I_b=-0.25$, and (b) the PRC for the Hodgkin-Huxley equations with standard parameters and $I_b=10$

esting to investigate the relationship between this feature-based approach and that taken in the present paper, especially because the dominant such feature identified for the HH equations in [23] resembles in form the optimal currents for these equations computed here.

We close by mentioning an alternative approach to the problem of complex neural inputs to the probabilistic approach taken in [12,23]: exploring the entire family of inputs $I(t)$ that elicit a spike at time t_1. The complement to this "level set" of inputs would then correspond to the (span of the) dominant features identified in [12,23]. This level-set-based approach was developed to answer related questions for other physical models in [24], and we have checked that the formalism extends readily to phase-reduced neuron models. As such, the optimal inputs studied in this paper may be viewed as distinguished points on the level set from which to begin this future analysis.

Acknowledgment

References

[1] Ashwin, P., and Swift, J., 1992, "The Dynamics of N Weakly Coupled Identical Oscillators," J. Nonlinear Sci., **2**, pp. 69–108.

[2] Brown, E., Holmes, P., and Moehlis, J., 2003, "Globally Coupled Oscillator Networks," in *Problems and Perspectives in Nonlinear Science: A Celebratory Volume in Honor of Lawrence Sirovich*, E. Kaplan, J. E. Marsden, and K. R. Sreenivasan, eds., Springer, New York, pp. 183–215.

[3] Cohen, A., Holmes, P., and Rand, R. H., 1982, "The Nature of Coupling Between Segmental Oscillators of the Lamprey Spinal Generator for Locomotion: A Model," J. Math. Biol., **13**, pp. 345–369.

[4] Gerstner, W., van Hemmen, L., and Cowan, J., 1996, "What Matters in Neuronal Locking?" Neural Comput., **8**, pp. 1653–1676.

[5] Ghigliazza, R. M., and Holmes, P., 2004, "A Minimal Model of a Central Pattern Generator and Motoneurons for Insect Loco-Motion," SIAM J. Appl. Dyn. Syst., **3**(4), pp. 671–700.

[6] Hansel, D., Mato, G., and Meunier, C., 1993, "Phase Dynamics for Weakly Coupled Hodgkin-Huxley Neurons," Europhys. Lett., **25**(5), pp. 367–372.

[7] Kopell, N., and Ermentrout, G. B., 1990, "Phase Transitions and Other Phenomena in Chains of Coupled Oscillators," SIAM J. Math. Anal., **50**, pp. 1014–1052.

[8] Taylor, D., and Holmes, P., 1998, "Simple Models for Excitable and Oscillatory Neural Networks," J. Math. Biol., **37**, pp. 419–446.

[9] Brown, E., Moehlis, J., and Holmes, P., 2004, "On the Phase Reduction and Response Dynamics of Neural Oscillator Populations," Neural Comput., **16**, pp. 673–715.

[10] Brown, E., Moehlis, J., Holmes, P., Clayton, E., Rajkowski, J., and Aston-Jones, G., 2004, "The Influence of Spike Rate and Stimulus Duration on Noradrenergic Neurons," J. Comput. Neurosci., **17**, pp. 13–29.

[11] Tass, P. A., 1999, *Phase Resetting in Medicine and Biology*, Springer, New York.

[12] Rieke, F., Warland, D., de Ruyter van Steveninck, R., and Bialek, W., 1996, *Spikes: Exploring the Neural Code*, MIT Press, Cambridge, MA.

[13] Forger, D. B., and Paydarfar, D., 2004, "Starting, Stopping, and Resetting Biological Oscillators: In Search of Optimal Perturbations," J. Theor. Biol., **230**, pp. 521–532.

[14] Tuckwell, H., and Feng, J., 2005, "Optimal Control of Neuronal Activity," Phys. Rev. Lett., **91**, p. 018101.

[15] Winfree, A., 2001, *The Geometry of Biological Time*, 2nd ed., Springer, New York.

[16] Bryson, A., and Ho, Y., 1975, *Applied Optimal Control*, Halsted Press, Washington, DC.

[17] Goldstein, H., 1980, *Classical Mechanics*, 2nd ed., Addison-Wesley, Reading, MA.

[18] Ermentrout, G. B., 1996, "Type I Membranes Phase Resetting Curves, and Synchrony," Neural Comput., **8**, pp. 979–1001.

[19] Ermentrout, G. B., and Kopell, N., 1984, "Frequency Plateaus in a Chain of Weakly Coupled Oscillators, I," SIAM J. Math. Anal., **15**, pp. 215–237.

[20] Hodgkin, A. L., and Huxley, A. F., 1952, "A Quantitative Description of Membrane Current and Its Application to Conduction and Excitation in Nerve," J. Physiol. (London), **117**, pp. 500–544.

[21] Ermentrout, G. B., 2002, *Simulating, Analyzing, and Animating Dynamical Systems: A Guide to XPPAUT for Researchers and Students*, SIAM, Philadelphia.

[22] Herrmann, A., and Gerstner, W., 2001, "Noise and the PSTH Response to Current Transients: I. General Theory and Application to the Integrate-and-Fire Neuron," J. Comput. Neurosci., **11**, pp. 135–151.

[23] Aguera y Arcas, B., Fairhall, A., and Bialek, W., 2003, "Computation in a Single Neuron: Hodgkin and Huxley Revisited," Neural Comput., **15**, pp. 1715–1749.

[24] Rothman, A., Ho, T.-S., and Rabitz, H., 2006, "Exploring Level Sets of Quantum Control Landscapes," Phys. Rev. A **73**, p. 053401.